Organic & Biomolecular Chemistry

Cite this: *Org. Biomol. Chem.*, 2011, **9**, 3733

www.rsc.org/obc

PAPER

Gas-phase ion-molecule reactions using regioselectively generated radical cations to model oxidative damage and probe radical sites in peptides†‡§

Christopher K. Barlow,[a,b,c] Adam Wright,[a,d] Christopher J. Easton[a,d] and Richard A. J. O'Hair*[a,b,c]

Received 24th December 2010, Accepted 22nd February 2011
DOI: 10.1039/c0ob01245a

Collision induced dissociation (CID) of sodiated peptide derivatives containing a nitrate ester functionality was used to regiospecifically generate three isomeric radicals of the model peptide Bz-Ala-Gly-OMe corresponding to radicals formed at: C^{α} of the alanine residue [**4**+Na]$^+$; C^{α} of the glycine residue [**5**+Na]$^+$; and the side chain of alanine [**6**+Na]$^+$. The ion-molecule reactions of these peptide radicals were examined to model oxidative damage to peptides and to probe whether the radical sites maintain their integrity or whether they isomerise *via* intramolecular hydrogen atom transfer (HAT). Only [**6**+Na]$^+$ is reactive towards O_2, forming the peroxyl radical [**7**+Na]$^+$, which loses O_2, HO$^{\bullet}$ and $HO_2^{\bullet}$ under CID. The radical ion [**7** + Na]$^+$ abstracts a hydrogen atom from 4-fluorothiophenol to form the hydroperoxide [**8**+Na]$^+$, which upon CID fragments *via* the combined loss of HO$^{\bullet}$ and CH_2O. In contrast, all three of the isomeric sodiated radicals react with NO$^{\bullet}$ and $NO_2^{\bullet}$ to form adducts. CID of the NO adducts only regenerates the radicals *via* NO$^{\bullet}$ loss, thus providing no structural information. In contrast, CID of the NO_2 adducts gives rise to a range of product ions and the spectra are different for each of the three adducts, suggesting that the isomeric radicals [**4**+Na]$^+$, [**5**+Na]$^+$ and [**6**+Na]$^+$ are produced as discrete species. Finally, CID of the NO_2 adducts was used to probe the rearrangement of the radicals [**4**+Na]$^+$, [**5**+Na]$^+$ and [**6**+Na]$^+$ prior to their reaction with $NO_2^{\bullet}$: [**6** + Na]$^+$ rearranges to a mixture of [**4**+Na]$^+$ and [**5**+Na]$^+$ while [**5**+Na]$^+$ rearranges to [**4**+Na]$^+$.

Introduction

In a fascinating in-depth interview,[1] Beckwith noted his interest in the roles of radicals in biology: *"One of the things I used to ask my students was, 'Why don't we go rancid?' It's a good question. Our bodies contain lots of fat. If one leaves a bit of fat lying out in the sun for a couple of days, it smells to high heaven. Why don't you and I go rancid? Well, we now know that fats go rancid because of free radical attack. Indeed, free radicals are everywhere. Whenever a chemical bond is broken by ultraviolet light, cosmic rays or beta radiation free radicals are formed. So radicals are ubiquitous. When they attack fats oxidative processes involving oxygen occur. The reason we don't go rancid is that we are protected while we are alive by natural anti-oxidants such as vitamin E and vitamin C. Because of this I became very interested in the mechanisms of metabolic reactions possibly involving the attack of radicals on the constituents of living organisms."*

Although Beckwith did not study oxidative damage of peptides and proteins induced by reactive oxygen species (ROS), it is now well established that attack by hydroxyl radicals, which are amongst the most reactive ROS species, can lead to permanent modification of proteins, especially at aromatic residues.[2] This can result in the formation of 3,4-dihydroxytyrosine, loss of tryptophan residues and cross-linking. Such modifications may substantially alter protein polarity and lead to loss of higher-order structure, making the proteins more susceptible to enzymatic degradation.[3] Hydroxyl radicals also react with proteins *via* hydrogen atom abstraction, leading to reactive species such as carbon-centred radicals, which undergo further reaction in the presence of molecular oxygen, ultimately leading to protein fragmentation.[3] Oxidative damage to proteins has been linked to a number of biological processes, including ageing and in Alzheimer's disease.[4] Recently it has been shown that nitric oxide (NO$^{\bullet}$) and nitroxide radicals can act as protective agents or "radical scavengers" by intercepting protein derived radicals.[5]

The chemical mechanisms associated with oxidative damage have been extensively examined and reviewed.[6,7] While much of the chemistry of simpler chemical systems is now understood from studies involving product analysis and EPR spectroscopy,

[a]*ARC Centre of Excellence for Free Radical Chemistry and Biotechnology, http://www.freeradical.org.au/. E-mail: rohair@unimelb.edu.au; Fax: +613 9347-5180; Tel: +61 3 8344-2452*
[b]*School of Chemistry, University of Melbourne, Victoria, 3010, Australia*
[c]*Bio21 Molecular Science and Biotechnology Institute, University of Melbourne, Victoria, 3010, Australia*
[d]*Research School of Chemistry, Australian National University, ACT 0200, Australia*

† Dedicated to the memory of Professor Athel Beckwith, an important pioneer of free radical chemistry and a giant in Organic Chemistry in Australia

‡ Part 79 of the series "Gas-Phase Ion Chemistry of Biomolecules"

§ Electronic supplementary information (ESI) available. See DOI: 10.1039/c0ob01245a

significant challenges arise in trying to examine mechanistic aspects in more complex molecules. This is due to a number of factors, including: (i) oxidative damage inflicted on proteins in the presence of oxygen may involve chain processes that damage significantly more sites than the initial site of radical production;[3,8] and (ii) many of the intermediate species are highly reactive-for example peroxyl radicals formed *via* addition of O_2 to peptide or protein radicals only have short lifetimes in aqueous solution and readily undergo a range of reactions.[9,10] The structure and chemistry of peroxyl radicals of small model peptides have been the subject of several experimental studies[11,12] and a theoretical report.[13] These peroxyl radicals can undergo a number of subsequent bimolecular and unimolecular reactions including fragmentation *via* intramolecular hydrogen atom transfer (HAT) followed by expulsion of $HO_2^{\bullet}$, as illustrated for glycine anhydride in Scheme 1.[11]

Mass spectrometry (MS) has played an important role as an analytical tool to interrogate the oxidation products of biological systems[14] including peptides.[15] Beyond the analytical role for MS, which typically involves the examination of the even-electron end products, there has been considerable interest in using MS-based methods to examine the fundamental gas-phase unimolecular and bimolecular reactivity of charged radical (odd electron) reactive intermediates of peptides.[16–29] We have previously utilised the sodiated nitrate ester derivatives [**1**+Na]$^+$–[**3**+Na]$^+$ (Scheme 2) to generate sodiated radicals of the model peptide Bz-Ala-Gly-OMe *via* low energy collision induced dissociation (CID).[19] CID results in the loss of $NO_2^{\bullet}$ and CH_2O to afford the corresponding radical ions [**4**+Na]$^+$–[**6**+Na]$^+$, shown in Scheme 2. These radicals may be considered as models for the simple dipeptide sequence Ala-Gly undergoing hydrogen atom abstraction to produce radicals at the following sites: C^{α} of the alanine residue [**4**+Na]$^+$; C^{α} of the glycine residue [**5**+Na]$^+$; and the side-chain of alanine [**6**+Na]$^+$. An important consequence of this method of generating peptide radicals is that the site at which the radical is formed is predetermined by the location of the nitrate ester moiety. The sodium cation was chosen as "charge handle" to allow for manipulation and analysis *via* mass spectrometry based methods. The sodium cation has been previously shown to bind to the carbonyl oxygens of the amide and carboxylate groups of related peptides[30] and is not expected to play a significant role in the formation and reactions of the radical cation.

We found that each of these different radicals [**4**+Na]$^+$–[**6**+Na]$^+$ gave a virtually identical low energy CID spectrum, suggesting that the radicals interconvert prior to fragmentation. This observation is consistent with the results of DFT calculations, which revealed that the barriers for intramolecular HAT are less than the energy required to fragment the peptide. Since then, there has been significant interest in whether HAT is a general phenomenon in the unimolecular chemistry of peptide radical ions.[22,26–29] As CID has the potential to cause migration of a radical site, developing alternative ways of probing radical sites in peptides is highly desirable. Ion-molecule reactions have been used to probe the radical environments in organic distonic ions[31] and have been recently applied to examine radical sites in amino acid and peptide radical ions.[19,29,32] For example, we have shown that a β-alanyl radical reacts with allyl iodide and dimethyl disulfide, whereas the isomeric α-alanyl radical is unreactive towards these reagents.[19] More recently, Moore *et al.*,[29] have used ion-molecule reactions of peptide radical ions with oxygen to explore the issue of radical migration.

Given Beckwith's interest in the chemistry of peroxyl radicals, which date back to his early studies on the radical reactions of anthracenes in the presence of thiols and oxygen[33,34] and his subsequent studies on the rearrangement reactions of peroxyl radicals derived from lipids,[35,36] we thought it would be fitting to report on our studies on the ion-molecule reactions of the three isomeric sodiated peptide radicals [**4**+Na]$^+$–[**6**+Na]$^+$, shown in Scheme 2, with O_2, $NO^{\bullet}$ and $NO_2^{\bullet}$. Our aims for this work were to: (i) establish whether these peptide radicals react with oxygen in the gas phase to form peroxyl radicals, and if so to examine the gas-phase chemistry of these peroxyl radicals; and (ii) determine if the radicals $NO^{\bullet}$ and $NO_2^{\bullet}$ can act as "radical scavengers" of these peptide radicals, and if so to establish whether the resultant adducts provided structural information on any migrations of the original peptide radical sites.

Experimental

Materials

Seeded He bath gas: 1.05 ± 0.03% mole O_2 in He and 1.02% mole NO in He were purchased from Air Liquide Australia Ltd., Melbourne, Australia. 871 ± 17 ppm O_2 in He was purchased from BOC Gases Australia Ltd., Melbourne, Australia. 4-Fluorothiophenol was purchased from Sigma–Aldrich Chemical Co., Australia and used without further purification. All solvents were reagent grade and used without further purification.

Synthesis of the nitrate esters 1–3

The nitrate esters **1–3** were prepared using the general methods previously reported.[19,37,38] They were characterized *via* a range of techniques including ^{1}H NMR spectroscopy (Varian Gemini 300 and Varian Inova 500 spectrometers), ESI mass spectrometry (Micromass-Waters LC-ZMD single quadrupole liquid chromatograph and Thermo-Finnigan LTQ-FT mass spectrometers) and elemental analysis (Australian National University Analytical Services Unit).

N-Benzoyl-*O*$^{\beta}$-nitro-α-methylserylglycine methyl ester **1**: mp 124–126 °C (from ethyl acetate/hexane). Found: C, 49.63; H, 5.10; N, 12.48. $C_{14}H_{17}N_3O_7$ requires C, 49.56; H, 5.05; N, 12.38%. ^{1}H NMR: δ_H ($CDCl_3$) 1.56 (s, 3 H), 3.79 (s, 3 H), 4.95 (s, 2 H), 4.23 (m, 2 H), 7.10 (br m, 2 H), 7.45–7.80 (m, 5 H). MS (ESI) *m/z*: 362 M+Na]$^+$, 15%; 340 [M+H]$^+$, 100%; 277 [M–NO_2]$^+$, 65%.

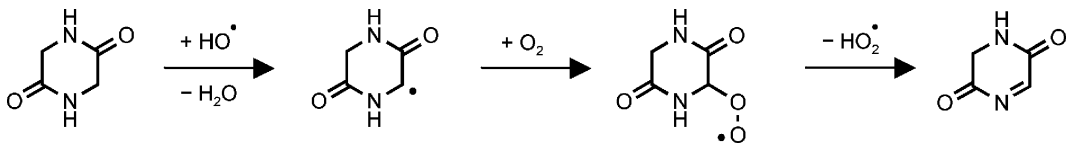

Scheme 1 Formation and fragmentation of a model peptide peroxyl radical (ref. 11).

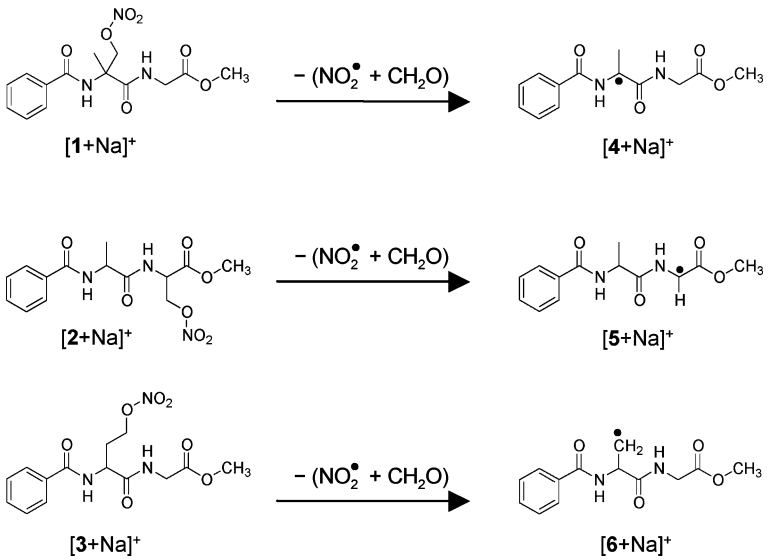

Scheme 2 Regioselective formation of the sodiated radical ions [**4**+Na]$^+$–[**6**+Na]$^+$, *via* the loss of $NO_2^{\bullet}$ and CH_2O from serine and homoserine nitrate ester derivatives [**1**+Na]$^+$–[**3**+Na]$^+$. Sodium ions have been excluded from structures for clarity.

N-Benzoyl-O^{β}-nitroalanylserine methyl ester **2**: mp 101–104 °C (from ethyl acetate/hexane). Found: C, 49.72; H, 5.03; N, 12.30. $C_{14}H_{17}N_3O_7$ requires C, 49.56; H, 5.05; N, 12.38%. ^{1}H NMR: δ_H ($CDCl_3$) 1.47 (d, *J* 6.5, 3 H), 3.82 (s, 3 H), 4.84 (m, 3 H), 4.92 (m, 1 H), 6.90 (br m, 2 H), 7.40–7.80 (m, 5 H). MS (ESI) *m/z*: 362 [M+Na]$^+$, 45%; 340 [M+H]$^+$, 100%; 277 [M–NO_2]$^+$, 35%.

N-Benzoyl-O^{γ}-nitrohomoserylglycine methyl ester **3**: mp 86–88 °C (from ethyl acetate/hexane). Found: C, 49.44; H, 4.97; N, 12.42. $C_{14}H_{17}N_3O_7$ requires C, 49.56; H, 5.05; N, 12.38%. ^{1}H NMR: δ_H ($CDCl_3$) 2.25 (m, 1 H), 2.40 (m, 1 H), 3.74 (s, 3 H), 4.06 (m, 2 H), 4.63 (m, 2 H), 4.92 (m, 1 H), 7.06 (br m, 2 H), 7.42–7.83 (m, 5 H). MS (ESI) *m/z*: 362 [M+Na]$^+$, 20%; 340 [M+H]$^+$, 100%; 277 [M–NO_2]$^+$, 20%.

Gas-phase formation of the sodiated peptide radicals [4+Na]$^+$–[6+Na]$^+$

The sodiated peptide nitrate ester ions [**1**+Na]$^+$–[**3**+Na]$^+$ were introduced into the gas-phase by dissolving a small amount (< 1 mg) of the corresponding peptide derivative in methanol and subjecting this solution (with a concentration of approximately 0.1 mmol) to electrospray ionization. There was no need to add a source of sodium cations to the ESI solution as adventitious sodium from the glass vials used to store the peptide nitrate esters was sufficient to give abundant [M+Na]$^+$. Alternatively, MeOD was used as the solvent to facilitate the exchange of the amide protons for deuterons. The sodiated peptide nitrate esters [**1**+Na]$^+$–[**3**+Na]$^+$ were then isolated in the ion trap and subjected to collision induced dissociation (CID), leading to the loss of $NO_2^{\bullet}$ and CH_2O to afford the corresponding radical ions [**4**+Na]$^+$–[**6**+Na]$^+$ shown in Scheme 2.

Mass spectrometry and ion-molecule reactions

Most experiments were performed in the linear ion trap of a commercially available hybrid quadrupole linear ion trap/Fourier transform ion cyclotron resonance mass spectrometer (Thermo-Finnigan model LTQ-FT, Bremen, Germany). Neutral reagents $NO^{\bullet}$ and O_2 were introduced into the ion trap using He bath gases that were seeded with a small concentration (between 0.01 and 1%) of the neutral reagent (see materials section above). Introduction of the $NO^{\bullet}$/He gas mixture into the ion trap also leads to $NO_2^{\bullet}$ formation *via* the reaction of $NO^{\bullet}$ with adventitious oxygen. Alternatively, in some cases it was desirable to conduct experiments with a higher concentration of $NO_2^{\bullet}$ in the ion trap. This was achieved by flushing the ion trap manifold with 1% O_2 seeded bath gas for 30–60 min before switching to $NO^{\bullet}$ seeded bath gas. This provided sufficient $NO_2^{\bullet}$ to conduct ion-molecule reactions (IMRs) for several hours. The accurate masses of products arising from IMRs and further CID were determined by high-resolution mass spectrometry, in which ions from the linear ion-trap were transferred to the FT-ICR cell.

IMRs with 4-fluorothiophenol were carried out on a quadrupole ion trap mass spectrometer (Finnigan-MAT model LCQ, San Jose, CA, USA), which has been modified to allow the introduction of less volatile neutral reagents into the ion trap *via* a side-arm.[39,40]

Ion manipulation

Experiments described here involve several steps of isolation, CID and IMRs. Furthermore, the results obtained often depend critically upon the details of the scan function described. All stages of ion isolation, storage, CID *etc.* were controlled using the Xcalibur software. All IMRs and CID were conducted using the default resonant excitation q (Q) value of 0.25, while other parameters namely the parent mass (*m/z*), isolation width (w), normalised collision energy (NCE) and activation time (*t* (ms)) were varied. Details of the scan parameters accompany all spectra using a nomenclature based on that described previously by Cooks and co-workers.[41]

The rate of O_2 addition to [6+Na]$^+$

A known concentration of O_2 was introduced into the ion trap *via* the use of a He bath gas cylinder seeded with O_2. During

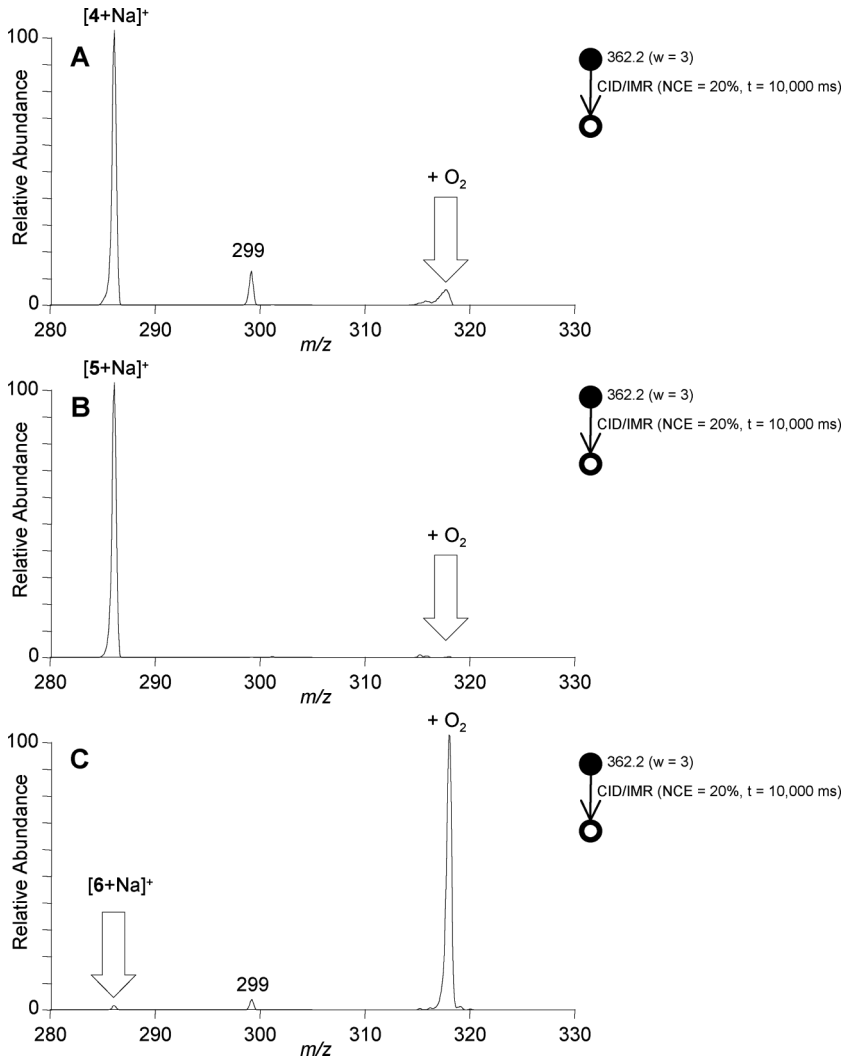

Fig. 1 The MS obtained following CID of [**1**+Na]$^+$ (A), [**2**+Na]$^+$ (B) and [**3**+Na]$^+$ in the presence of ~1% O_2 for a period of 10 s. There is little or no addition of O2 to [**4**+Na]$^+$ or [**5**+Na]$^+$, in contrast virtually all of [**6**+Na]$^+$ has reacted to form the corresponding O_2 adduct. Note, ions at *m/z* 299 correspond to the loss of HNO_3 from the parent nitrate ester.

the exchange of these cylinders air enters the vacuum system and thus the amount of background oxygen is unknown. As a consequence, rate experiments were not recorded immediately following the exchange of cylinders. Instead, the instrument was left for approximately 12 h to allow the partial pressure of O_2 to equilibrate. Addition of O_2 is measured in an MS^3 experiment. In the first step the sodiated nitrate ester [**3**+Na]$^+$ is isolated (w = 3.0) and subjected to CID (*m/z* 362.2, NCE = 20%, Q = 0.25, *t* = 30 ms) in order to form the corresponding sodiated radical [**6**+Na]$^+$, which is then isolated (w = 5.0) and trapped (*m/z* 286.0, NCE = 0%, Q = 0.25) for a period *t* (ms), followed by scan out to record the product ion mass spectrum.

Results and discussion

(1) Reactivity of peptide radicals towards O_2

Comparisons of reactions of [4+Na]$^+$, [5+Na]$^+$ and [6+Na]$^+$ with dioxygen. Given that previous studies have shown that charged peroxyl radicals can be formed in the gas phase *via* O_2 addition to distonic ions,[29,42–45] we were interested in comparing the reactivity of the isomeric radicals [**4**+Na]$^+$, [**5**+Na]$^+$ and [**6**+Na]$^+$ towards dioxygen. Fig. 1 shows the MS^2 spectra following CID of the sodiated nitrate esters [**1**+Na]$^+$, [**2**+Na]$^+$ and [**3**+Na]$^+$ using He bath gas seeded with ~1% O_2 for 10 s. Trapping the C^α-centred radicals [**4**+Na]$^+$ and [**5**+Na]$^+$ leads to little or no addition (Fig. 1A and B). In contrast, an examination of Fig. 1C reveals that the less stable primary alanyl side-chain radical [**6**+Na]$^+$ adds dioxygen to form a peroxyl radical. The rate of this addition is slow ($2.4 \pm 0.5 \times 10^{-12}$ cm^3 molecule^{-1} *sec*$^{-1}$) with a reaction efficiency of about 0.5% (see Supplementary material for a detailed discussion on these measurements).[46] The differences in reactivity of the three radicals [**4**+Na]$^+$–[**6**+Na]$^+$ suggest that they maintain their integrity prior to oxygen exposure and CID, and is also consistent with our previous studies, which showed that β-alanyl radicals are more reactive towards allyl iodide and dimethyl disulfide than α-alanyl radicals.[19] The relative reactivity of the two types of radicals is also consistent with the greater stability of C^α-radicals due to the captodative stabilisation afforded by the adjacent amide nitrogen and carbonyl groups.[47] Indeed previous high level

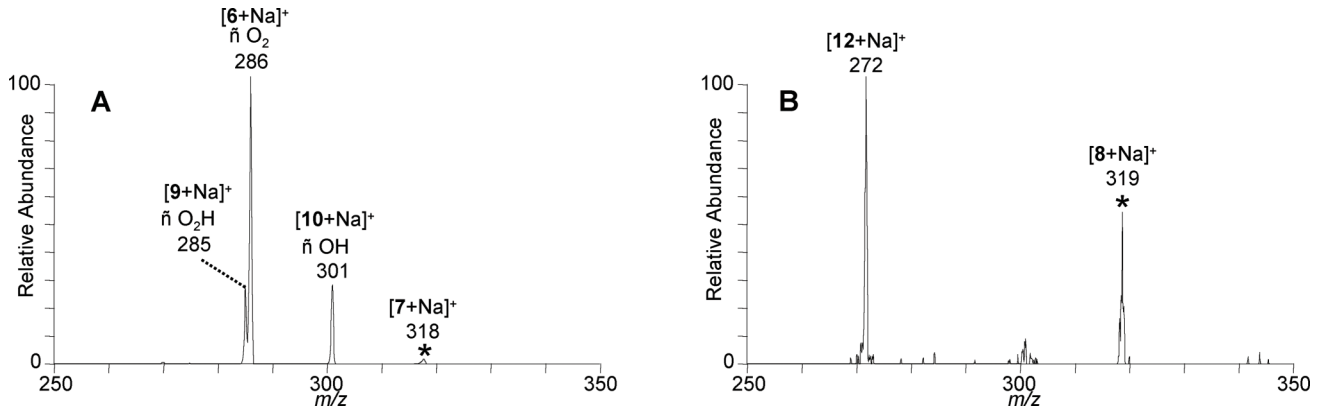

Fig. 2 CID spectrum of the peroxyl radical [**7**+Na]$^+$, formed upon addition of O_2 to [**6**+Na]$^+$. **B**. CID spectrum of the hydroperoxide [**8**+Na]$^+$, which was formed *via* hydrogen atom transfer from 4-fluorothiophenol to the peroxyl radical [**7**+Na]$^+$ (conducted using a modified LCQ to allow the introduction of 4-fluorothiophenol).

computational studies (at the RMP2(riv)/G3MP2Large//B3-LYP/6-31G(*d*) level of theory) of these sodiated peptide radicals provided the following relative energies: [**4**+Na]$^+$ (0.0) < [**5**+Na]$^+$ (+18.1 kJ mol^{-1}) < [**6**+Na]$^+$ (59.4 kJ mol^{-1}).[19]

Failure to observe significant addition of O_2 to the C$^\alpha$-radicals is counter to the prevailing belief that related protein radicals react close to the diffusion controlled limit with O_2 [7] and also appears to be inconsistent with recent solution phase studies, where peroxyl radicals derived from *N*-acetylglycine and diglycine were observed at room temperature *via* time-resolved EPR spectroscopy.[12] A possible explanation is that in the gas phase these exothermic reactions are reversible (eqn (1) and (2)) and that unless the resultant peroxyl radical can either be collisionally stabilised or undergo intramolecular HAT to form a new radical (eqn (3)), then the peroxyl radical will dissociate back to the parent peptide radical.

$$R^{\bullet} + O_2 \rightarrow RO_2^{\bullet} \quad (1)$$

$$RO_2^{\bullet} \rightarrow R^{\bullet} + O_2 \quad (2)$$

$$RO_2^{\bullet} \rightarrow (R{-}H^{\bullet})O_2H \quad (3)$$

The fact that [**4**+Na+O_2]$^+$ and [**5**+Na+O_2]$^+$ may not be able to undergo intramolecular HAT to form a new radical, whereas [**6**+Na+O_2]$^+$ may, appears to be supported by CID studies on [**6**+Na+O_2]$^+$ (see section below) and by thermochemical estimates from a theoretical study.[13] Thus using the C$^\alpha$-radicals of *N*-formylglycinamide and *N*-formylalaninamide as models, eqn (1) is predicted to be exothermic by 89 and 86 kJ mol^{-1}, respectively, but this energy cannot be used to fuel HAT of the peroxyl radicals to the corresponding aminyl (*N*-centered) radicals (eqn (3)), which is predicted to be endothermic by 106 and 97 kJ mol^{-1}, respectively. Thus there is an energy deficit (eqn (3) – eqn (1)) of 17 kJ mol^{-1} in the case of *N*-formylglycinamide and 11 kJ mol^{-1} in the case of *N*-formylalaninamide. In contrast, formation of the side chain peroxyl radical [**6** + Na + O_2]$^+$ is expected to be much more exothermic (eqn (1)) and HAT of the peroxyl radical (eqn (3)) to other positions (*e.g.* to form a stable C$^\alpha$ radical) is expected to be no more endothermic and thus there is unlikely to be an overall energy deficit.¶

Unimolecular and bimolecular reactivity of the peroxyl radical [6+Na+O_2]$^+$. Although the solution-phase chemistry of peroxyl radicals formed on peptides is complex, they are known to decompose to carbonyl compounds, alcohols or alkoxyl radicals.[2] CID of the peroxyl radical [**7**+Na]$^+$, formed upon addition of O_2 to [**6**+Na]$^+$, leads primarily to the loss of O_2 (Fig. 2A), confirming that the addition of O_2 to the peptide radical is reversible (eqn (2)). The two other minor reaction channels are important since they provide evidence for rearrangement *via* intramolecular HAT (eqn (3)). They involve the elimination of HO$^\bullet$ and $HO_2^\bullet$ presumably to afford the aldehyde [**10**+Na]$^+$ and the dehydroalanine derivative [**9**+Na]$^+$, respectively (Fig. 2A, Scheme 3).‖

A major fate of peroxyl radicals in solution is abstraction of a hydrogen atom from hydrogen atom donors (*e.g.*, solvent) to form the corresponding hydroperoxides, which may then undergo further decomposition. In order to investigate such processes, a second neutral reagent was introduced into the ion trap along with O_2, using a specially modified LCQ (3D ion trap instrument).[39,40] Isolation of [**7**+Na]$^+$ in the presence of 4-fluorothiophenol led to formation of a small amount of the corresponding hydroperoxide [**8**+Na]$^+$, although this reaction was very slow (data not shown).** CID of [**8**+Na]$^+$ leads predominantly to an ion at *m/z* 272 (Fig. 2B and Scheme 3). We propose that this occurs *via* loss of HO$^\bullet$ to form an intermediate alkoxyl radical [**11**+Na]$^+$, which is not directly observed but rapidly undergoes β-scission to eliminate CH_2O and generate the C$^\alpha$-centred radical [**12**+Na]$^+$ (Scheme 3). Such a reaction sequence is directly analogous to the losses of $NO_2^\bullet$ and CH_2O from the nitrate ester [**3**+Na]$^+$ (Scheme 2).

¶ The ROO-H bond dissociation energy (BDE) is around 365 kJ mol^{-1},[48] while the C-H BDE for the α position of glycyl residues is around 340 kJ mol^{-1}.[48]

‖ Alternatively an expoxide might be formed instead of an aldehyde.[45]

** This reaction is expected to be exothermic: the ROO-H BDE is around 365 kJ mol^{-1},[48] while the thiophenol S-H BDE is around 335 kJ mol^{-1}.[48]

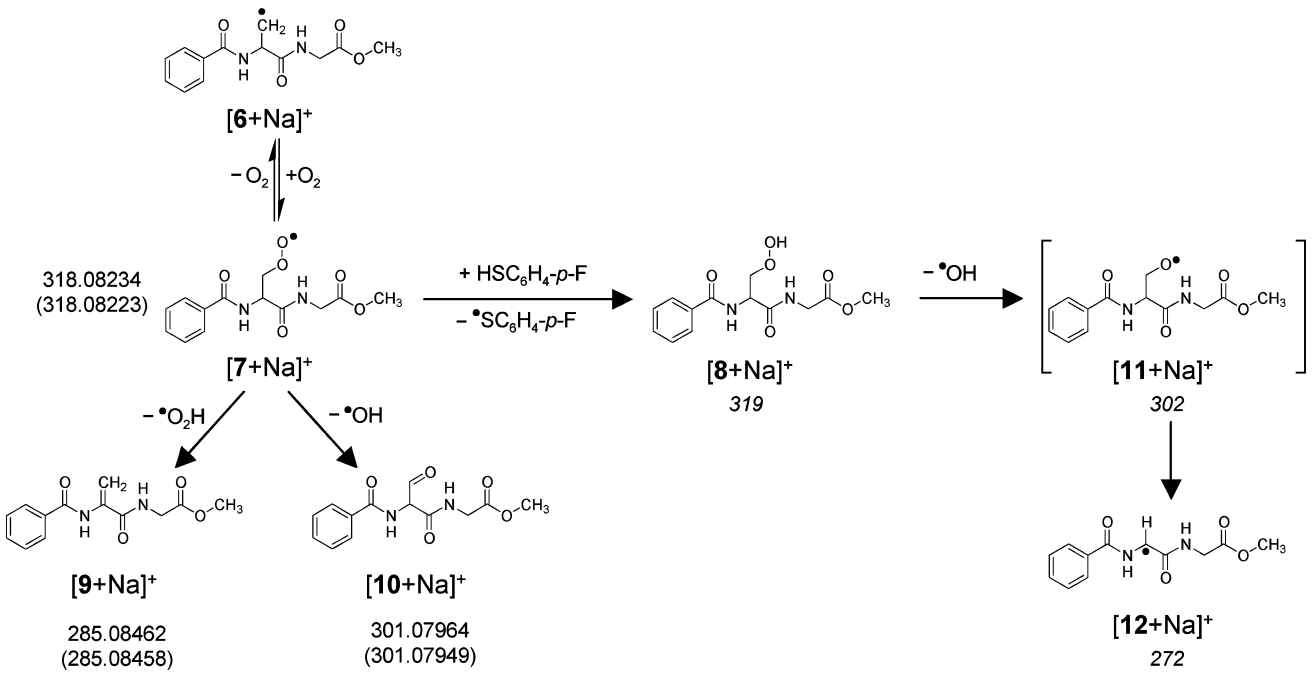

Scheme 3 Reaction scheme showing the formation and subsequent decomposition of the peroxyl radical [**7**+Na]$^+$ and the hydroperoxide [**8**+Na]$^+$. Experimental high resolution masses are given along with the corresponding theoretical masses in parentheses. Where it was not possible to record a high resolution mass (*i.e.*, LCQ experiments) the integer mass is provided. Sodium ions have been excluded from structures for clarity.

(2) Reactivity of peptide radicals towards NO$^\bullet$ and NO_2

Addition of NO$^\bullet$ and $NO_2^\bullet$ to [4+Na]$^+$, [5+Na]$^+$ and [6+Na]$^+$. Although the IMRs with O_2 allowed differentiation of the side chain radical [**6**+Na]$^+$, from the C$^\alpha$radicals [**4**+Na]$^+$ and [**5**+Na]$^+$, we were interested in developing more reactive reagent gases as probes of all three radical sites in our peptide model (Scheme 2). Since nitric oxide and nitroxides have been used as protein "radical scavengers" in *solution*,[5] we next explored the use of NO$^\bullet$ and $NO_2^\bullet$ to probe peptide radical structure in the *gas phase*. The spectra resulting from CID of the sodiated nitrate esters [**1**+Na]$^+$, [**2**+Na]$^+$ and [**3**+Na]$^+$, using He bath gas seeded with ~1% NO are shown in Fig. 3. It is clear that the CID radical products at *m/z* 286 are highly reactive towards this bath gas mixture (which contains a mixture of NO$^\bullet$ and $NO_2^\bullet$ -see below) and give rise to a range of products. Thus [**4**+Na]$^+$, [**5**+Na]$^+$ and [**6**+Na]$^+$ all rapidly undergo the addition of NO$^\bullet$ and $NO_2^\bullet$ to afford product ions at *m/z* 316 and 332.

While the relative intensities of the NO and NO_2 adducts varies in the three spectra shown in Fig. 3, differences in the relative concentrations of NO$^\bullet$ and $NO_2^\bullet$ are expected to be significant due to the *in situ* nature of $NO_2^\bullet$ formation *via* reaction of NO$^\bullet$ with adventitious O_2. For example, immediately following exchange of the He bath gas cylinder for the corresponding He/NO$^\bullet$ seeded cylinder significantly more $NO_2^\bullet$ addition was observed than NO$^\bullet$ addition. For experiments conducted some time after the cylinders had been exchanged, $NO_2^\bullet$ addition diminished in favor of NO$^\bullet$ addition (data not shown). This is consistent with oxygen entering the vacuum system during the cylinder exchange but decreasing in concentration by reacting over time. Consequently the relative rates of addition of NO$^\bullet$ or $NO_2^\bullet$ cannot be reliably established in our experiments. Nonetheless, since NO and NO_2 adducts are readily formed, we next turned our attention to examining the fragmentation behaviour of these adducts under CID conditions.

CID of the NO and NO_2 adducts of [4+Na]$^+$, [5+Na]$^+$ and [6+Na]$^+$. CID of the nitrosylated peptides formed upon addition of NO$^\bullet$ leads almost exclusively to loss of NO$^\bullet$ to regenerate the initial radical. For example, Fig. 4 shows the CID of the NO$^\bullet$ addition product of [**4**+Na]$^+$. In contrast, the CID spectra of the nitrite esters formed following addition of $NO_2^\bullet$ are significantly more complex and are described in detail below for each individual peptide radical isomer.††

CID of [4+Na+NO_2]$^+$. The CID spectrum of the nitrite ester [**13**+Na]$^+$, formed following addition of $NO_2^\bullet$ to [**4**+Na]$^+$, is shown in Fig. 5A. Only two product ions are observed at *m/z* 285 and 186. The former ion arises from loss of NO_2H, as confirmed by high-resolution measurements (see Scheme 4). Furthermore, exchange of the amide protons for deuterons results in the elimination of NO_2D (data not shown). This suggests that the product at *m/z* 285 corresponds to the imine [**14**+Na]$^+$, formed *via* a pericyclic reaction. The product ion at *m/z* 186 is proposed to form *via* the initial loss of NO$^\bullet$ to generate a transient intermediate alkoxy radical [**15**+Na]$^+$, which is not observed but undergoes β-scission of the backbone C–C bond to afford *N*-acetylbenzamide [**16**+Na]$^+$.

†† We have tentatively assigned the NO_2 adducts to the nitrite ester structures shown in Schemes 4–6. We cannot, however rule out isomeric nitro structures, which have been predicted to be thermodynamically favoured for simple organic systems.[49]

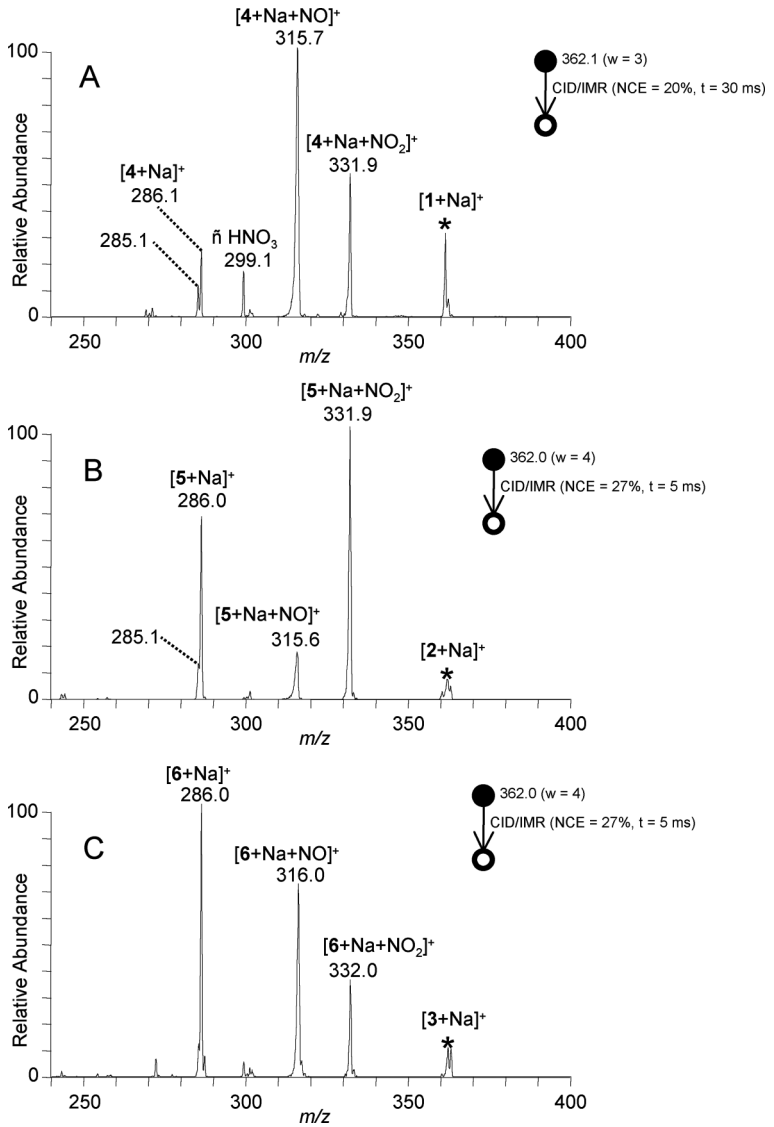

Fig. 3 CID spectra of [**1**+Na]$^+$–[**3**+Na]$^+$ (*m*/*z* 362) in the presence of NO and NO_2. The corresponding radical ions are formed at *m*/*z* 286. Other products correspond to the addition of NO (*m*/*z* 316) or NO_2 (*m*/*z* 332) and products corresponding to the further fragmentation of these ions.

CID of [5+Na+NO$_2$]$^+$. CID of [**17**+Na]$^+$, the nitrite ester formed upon addition of $NO_2^{\bullet}$ to [**5**+Na]$^+$, the C^{α}-glycyl radical, is shown in Fig. 5B and possible product ion structures are shown in Scheme 5. The primary product ion at *m*/*z* 285 corresponds to the loss of NO_2H and may be rationalized *via* a pericyclic reaction to yield the imine formed at the *C*-terminal residue [**19**+Na]$^+$. Loss of NO$^{\bullet}$ forms a short-lived alkoxyl radical intermediate which fragments *via* β-scission of the backbone C–C bond to afford the product ion [**20**+Na]$^+$ at *m*/*z* 243. In addition, product ions at *m*/*z* 301 and 244 are also formed. High-resolution measurements indicate that the ion *m*/*z* 301 corresponds to the elimination of HNO to yield the α-diketone [**18**+Na]$^+$, formed *via* abstraction of the C^{α}-proton. This assignment is consistent with experiments in which the amide protons are exchanged for deuterons (data not shown). The absence of HNO loss in the CID of [**13**+Na]$^+$ also supports this mechanism as in this case no C^{α}-proton is available. The identity of the product ion at *m*/*z* 244 is not immediately apparent. High-resolution measurements indicate the molecular formula of this ion is $C_{10}H_{11}N_3O_3Na$, which may arise *via* pericyclic retro-group-transfer reaction to yield [**21**+Na]$^+$.

CID of [6+Na+NO$_2$]$^+$. CID of [**22**+Na]$^+$, the nitrite ester formed upon addition of $NO_2^{\bullet}$ to the C-3 alanine side-chain radical [**6**+Na]$^+$, results in the most complex chemistry of all the three nitrite esters (Fig. 5C and Scheme 6). Loss of NO_2H is observed, although in this case the C^{α} might be expected to be the source of the proton rather than the amide.‡‡ Loss of HNO (*m*/*z* 301) can be readily rationalized to afford a side-chain aldehyde [**23**+Na]$^+$, with the proton originating from the β-carbon.

‡‡ The H/D exchange experiments in this case are complicated. We observe ions consistent with both the loss of NO_2H and NO_2D. Some loss of NO_2D may be accounted for by preliminary isomerization of [**6**+Na]$^+$ to either [**4**+Na]$^+$ or [**5**+Na]$^+$ prior to addition of $NO_2^{\bullet}$ (this is discussed in the following section). The possibility of H/D scrambling in intermediate ion-molecule complexes cannot be discounted.

β-Scission of the alkoxyl radical formed by loss of NO$^{\bullet}$ results in elimination of formaldehyde to afford a new C^{α}-radical with *m/z* 272 in which the side chain has been lost [**12**+Na]$^+$. Note that this is the same radical formed *via* loss of HO$^{\bullet}$ and CH_2O from [**8**+Na]$^+$ in Scheme 3. The resulting C^{α}-radical may then undergo further addition of NO$^{\bullet}$ or $NO_2^{\bullet}$ as confirmed by mass selecting [**12**+Na]$^+$ (supplementary Figure S3A). CID of the nitrate ester [**25**+Na]$^+$, formed by addition of $NO_2^{\bullet}$ to the radical [**12**+Na]$^+$, is shown in supplementary Figure S3B. The product ions arise *via* loss of: HNO, to afford an α-diketone [**26**+Na]$^+$; NO_2H to afford [**28**+Na]$^+$ and loss of NO followed by β-scission to give [**27**+Na]$^+$ as shown in Scheme 6.

Products are also evident at *m/z* 186, 243 and 244 in the CID spectrum of the *m/z* 332 shown in Fig. 5C. The formation of these ions from [**22**+Na]$^+$ is not readily rationalized, rather we suggest that prior to addition of $NO_2^{\bullet}$, a proportion of the [**6**+Na]$^+$ ion population undergoes isomerisation to the more stable C^{α}-centred radicals [**4**+Na]$^+$ and [**5**+Na]$^+$, since the corresponding nitrate esters formed upon $NO_2^{\bullet}$ addition to these radicals are known to provide product ions at *m/z* 186 and *m/z* 243 and 244, respectively

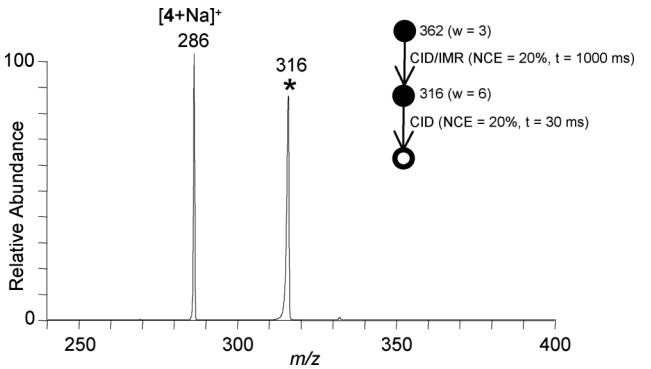

Fig. 4 CID of the NO addition product of [**4**+Na]$^+$, showing that loss of NO to regenerate the initial radical at *m/z* 286 is the primary reaction pathway.

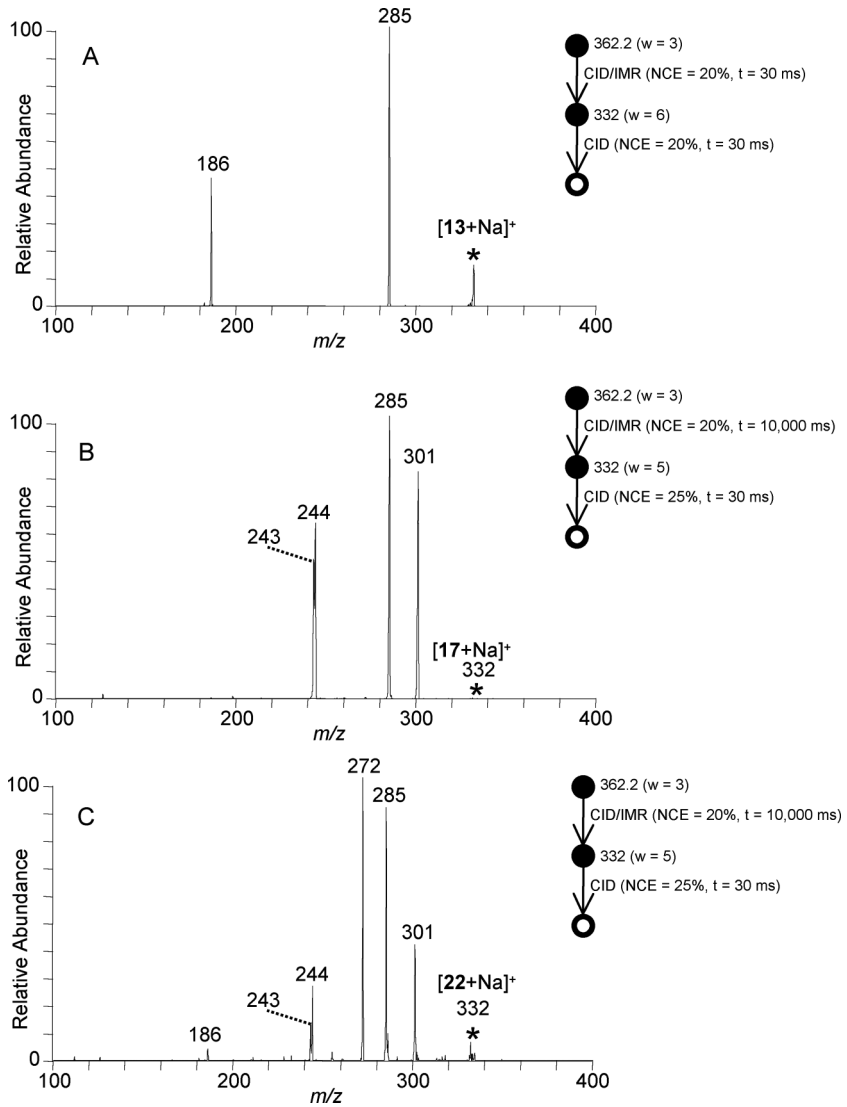

Fig. 5 Fragmentation of the nitrite esters formed following the addition of NO_2 to the radicals [**4**+Na]$^+$, [**5**+Na]$^+$ and [**6**+Na]$^+$. CID spectra of: **A** [**13**+Na]$^+$; **B** [**17**+Na]$^+$; and **C** [**22**+Na]$^+$.

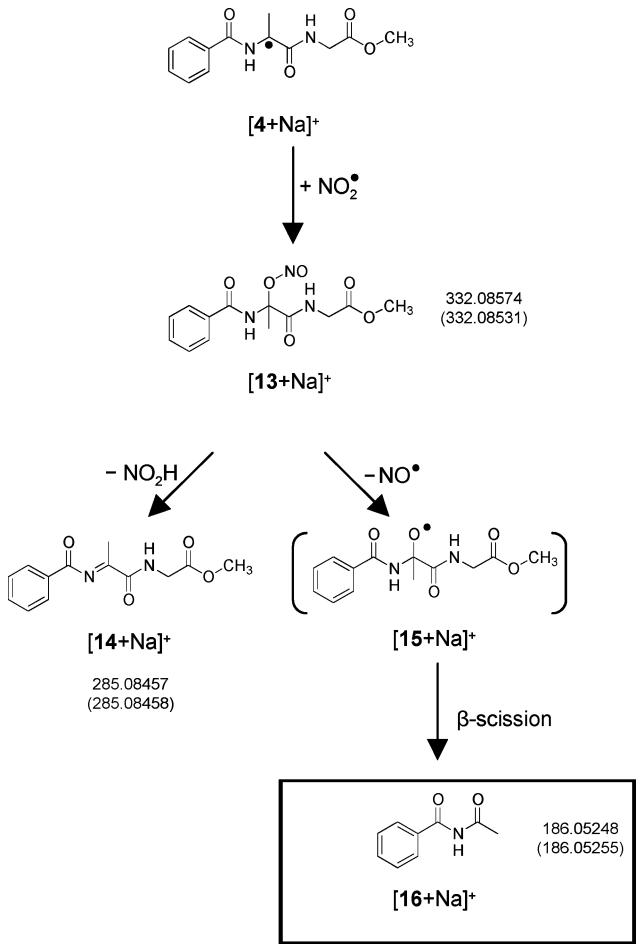

Scheme 4 Proposed fragmentation pathways for the nitrite ester [**13**+Na]$^+$ formed following addition of $NO_2^\bullet$ to [**4**+Na]$^+$. Experimentally observed high resolution masses are shown in plain text, theoretical masses are shown in parenthesis. Sodium ions have been excluded from structures for clarity. The fragment ion with an unique *m/z* value that is diagnostic of the [**4**+Na]$^+$ precursor is highlighted by a box.

(Fig. 5B and C and Schemes 4 and 5). The issue of isomerisation is explored further in the next section.

Using $NO_2^\bullet$ radical traps to probe the interconversion of [4+Na]$^+$, [5+Na]$^+$ and [6+Na]$^+$ *via* intramolecular HAT. The previously reported CID of the sodiated peptide radical cations [**4**+Na]$^+$, [**5**+Na]$^+$ and [**6**+Na]$^+$ provide spectra which are almost indistinguishable from each other. This led to the suggestion that isomerisation of the radical ions precedes fragmentation.[19] A key issue is whether these rearrangements occur spontaneously, or upon energizing the radical ions during CID. The spectra shown in Fig. 5 were recorded following initial isolation and CID of the nitrate esters [**X**+Na]$^+$ (X = **1–3**), which forms a product ion at *m/z* 286 as an intermediate, that in turn reacts during the MS^2 stage by addition of $NO_2^\bullet$ to provide a product ion at *m/z* 332. This [**X**+Na+NO_2]$^+$ (X = **4–6**) is then isolated and subjected to CID to give the MS^3 spectrum shown in Fig. 5X (X = A–C). Given that the CID spectra of each of these NO_2 adducts is sufficiently different (Fig. 5) and gives unique structurally diagnostic ions (see Schemes 4–6), this suggests that spontaneous isomerisation is minimal. To probe whether rearrangement can occur by gentle heating (*i.e.*, sufficient to induce rearrangement but not enough to cause fragmentation) prior to trapping of the radical by $NO_2^\bullet$, we have used an additional stage of mass spectrometry to isolate the radical intermediates at *m/z* 286 *prior* to addition of $NO_2^\bullet$. A series of test experiments in which the least stable radical [**6**+Na]$^+$ was mass selected with a range of different isolation widths and allowed to react with O_2 clearly show that the mere act of isolating [**6**+Na]$^+$ causes it to rearrange to the more stable radicals [**4**+Na]$^+$ and [**5**+Na]$^+$ (see Supplementary material Fig. S1 and associated discussion therein). While it is known that isolating ions in an ion trap can energize them (indeed fragile non-covalent complexes can only be mass selected using wide isolation "windows"[50]), this appears to be the first example of this causing a rearrangement reaction. Since the nitrate adducts allow distinction of the radical site (Fig. 5 and Schemes 4–6), we next carried out the same rearrangement reaction by mass selecting [**6**+Na]$^+$ and then probing the product(s) of rearrangement by allowing the ions at *m/z* 286 to undergo addition of $NO_2^\bullet$. The resultant nitrate adducts were mass selected and the CID spectrum is shown in Fig. 6A. An examination of this spectrum and a comparison to the CID spectrum of the nitrate ester directly formed from [**6**+Na]$^+$ (Fig. 5C and Scheme 6) shows a complete absence of the product ion at *m/z* 272, which is diagnostic of [**6**+Na]$^+$ (Scheme 6). Furthermore, the second generation product ions (*m/z* 318, 287, 271 or 172) arising from subsequent reactions of [**12**+Na]$^+$ with $NO_2^\bullet$ are entirely missing. Instead the spectrum shown in Fig. 6A appears to be a combination of the spectra observed upon CID of the nitrate esters formed from the C$^\alpha$-radicals [**4**+Na]$^+$ (Fig. 5A and Scheme 4) and [**5**+Na]$^+$ (Fig. 5B and Scheme 5).

Similar results were obtained upon addition of an isolation step for the glycyl C$^\alpha$-radical [**5**+Na]$^+$. For example, Fig. 6B and C show the CID spectra obtained in MS^4 experiments in which the radical is trapped at the MS^3 stage and allowed to react with $NO_2^\bullet$, followed by subsequent isolation and CID of the nitrate ester ions at *m/z* 332. The degree to which isomerisation occurs is sensitive to the isolation width used to isolate the radical intermediate at *m/z* 286. For example, the spectrum in Fig. 6B was recorded utilising an isolation width of 20 mass units and is characteristic of a mixture of [**13**+Na]$^+$ and [**17**+Na]$^+$ (evident by the *m/z* 186 product which is absent in Fig. 5B). The spectrum in Fig. 6C utilised a narrower isolation width of 3 in the MS^3 step. In this case the spectrum is nearly identical to that obtained for the CID of [**13**+Na]$^+$ (compare with Fig. 5A). Products at *m/z* 243, 244 and 301, which are characteristic of the fragmentation of [**17**+Na]$^+$ (see Fig. 5B) are only minor components, indicating that the initially formed [**5**+Na]$^+$ has almost completely isomerised to [**4**+Na]$^+$. The two spectra in Fig. 6B and C clearly indicate that the extent to which isomerisation occurs is critically dependent upon the isolation width utilised in the isolation of the radical species.

Attempts to induce isomerisation of the C$^\alpha$-alanine radical [**4**+Na]$^+$, in a similar fashion gave no evidence for the formation of either [**5**+Na]$^+$ or [**6**+Na]$^+$ (data not shown). The fact that [**6**+Na]$^+$ rearranges to a mixture of both [**4**+Na]$^+$ and [**5**+Na]$^+$ (Fig. 6A) and that [**5**+Na]$^+$ almost completely isomerises to [**4**+Na]$^+$ (Fig. 6A) suggests that [**4**+Na]$^+$ is the most stable of the three radicals examined. These experimental observations are consistent

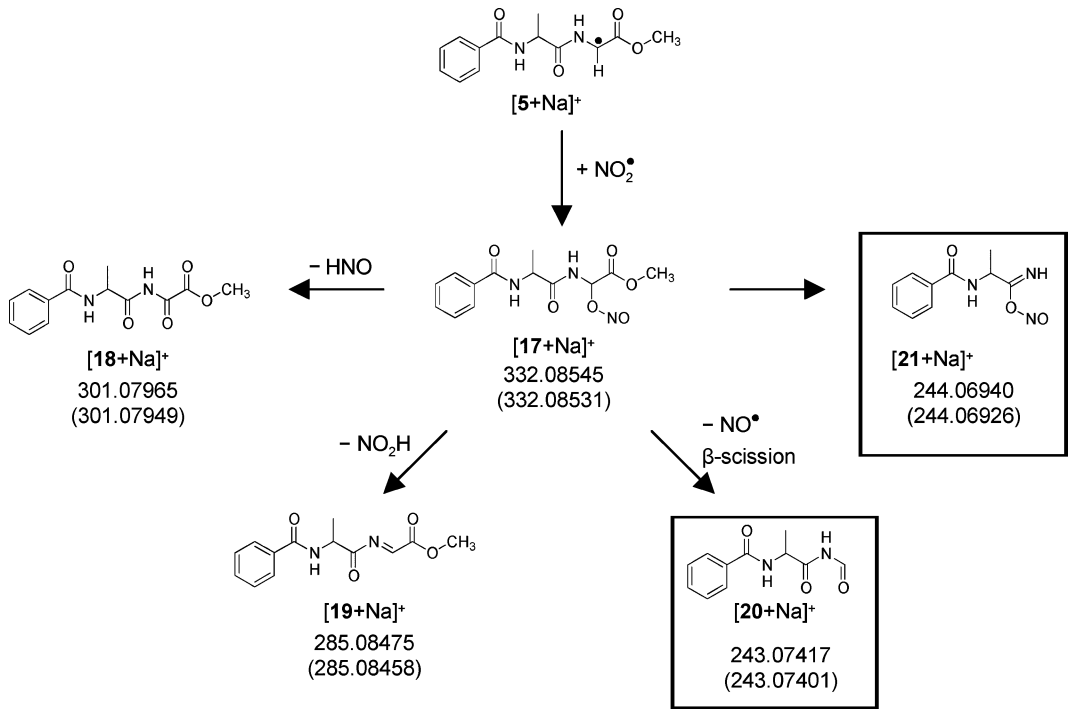

Scheme 5 Proposed structures of products formed upon CID of [**17**+Na]$^+$, which was formed by addition of $NO_2^{\bullet}$ to [**5**+Na]$^+$. Experimental accurate masses are given along with theoretical masses in parentheses. Sodium ions have been excluded from structures for clarity. The fragment ions with unique *m/z* values that are diagnostic of the [**5**+Na]$^+$ precursor are highlighted by boxes.

with previous theoretical calculations, which demonstrate that the relative energy of the radicals follows the order [**6**+Na]$^+$ > [**5**+Na]$^+$ > [**4**+Na]$^+$.[19]

(3) Intermediates of relevance to oxidative damage: gas-phase *versus* solution-phase chemistry

Although the mechanistic details associated with modification of peptide ions induced by ROS are complex, it is worth making some comparisons between known solution-phase chemistry and the gas-phase results presented in this study. In solution, initial attack by radical species on peptides or proteins predominantly leads to the formation of carbon-centred radicals either by addition to aromatic residues or hydrogen atom abstraction from C–H bonds at the backbone or side-chains. Related species can be formed in the gas phase by subjecting suitable ionic precursors to CID. In the present study we have used nitrate esters to regioselectively generate carbon-centred radicals (Scheme 2). In solution, the major fate of these C-centred radicals is either dimerisation in the absence of O_2 or addition to form peroxyl radicals in its presence.[2,7] In the gas phase, dimerisation is avoided (due to the fact that Coulomb repulsion will prevent two radical cations from reacting with each other), and thus the unimolecular and bimolecular reactivities of these radicals can readily be studied. While addition of O_2 to carbon-centred radicals is typically fast in solution, occurring close to the diffusion controlled limit,[7] we have found that the apparent rate of O_2 addition to peptide radicals may be substantially slower in the gas phase, with the C^{β}-alanine side-chain radical [**6**+Na]$^+$ reacting with an efficiency of around 0.5%. Furthermore addition of O_2 to the C^{α}-radicals [**4**+Na]$^+$ and [**5**+Na]$^+$ occurs at rates too slow to be effectively measured on the timescale of the experiments conducted here (ms to *sec*). A likely explanation is that these O_2 addition reactions are exothermic and reversible. In the dilute gas phase the resultant peroxyl radicals formed *via* eqn (1) remain energised and unless they can be collisionally cooled or rearrange to a new radical *via* intermolecular HAT (eqn (3)), they expel O_2 to reform the original C-centred radical (eqn (2)). In contrast, in solution the resultant peroxyl radical is surrounded by a complex environment (including solvent and other molecules). Solvent molecules can collisionally cool and thus stabilise the peroxyl radical, while other reactive molecules can react with the peroxyl radical to convert it to other species. Despite these differences, we have noted similarities in the subsequent unimolecular and bimolecular chemistry of the peroxyl radical:

(i) The peroxyl radical [**7**+Na]$^+$ fragments *via* losses of $HO^{\bullet}$ and $HO_2^{\bullet}$ (Scheme 3), processes that have analogues in the condensed phase (Scheme 1);

(ii) In solution, under conditions where the radical flux is low, a major fate of alkyl peroxyl radicals is to abstract a hydrogen atom from a suitable donor species to form an alkyl hydroperoxide species. We have successfully modeled this step by utilising 4-fluorothiophenol as a hydrogen atom donor (Fig. 2B and Scheme 3); and

(iii) In solution, decomposition of the peptide alkyl hydroperoxide *via* either one-electron reduction or cleavage of the peroxide bond results in the formation of an alkoxyl radical. Such species are known to undergo rapid β-scission when doing so affords a

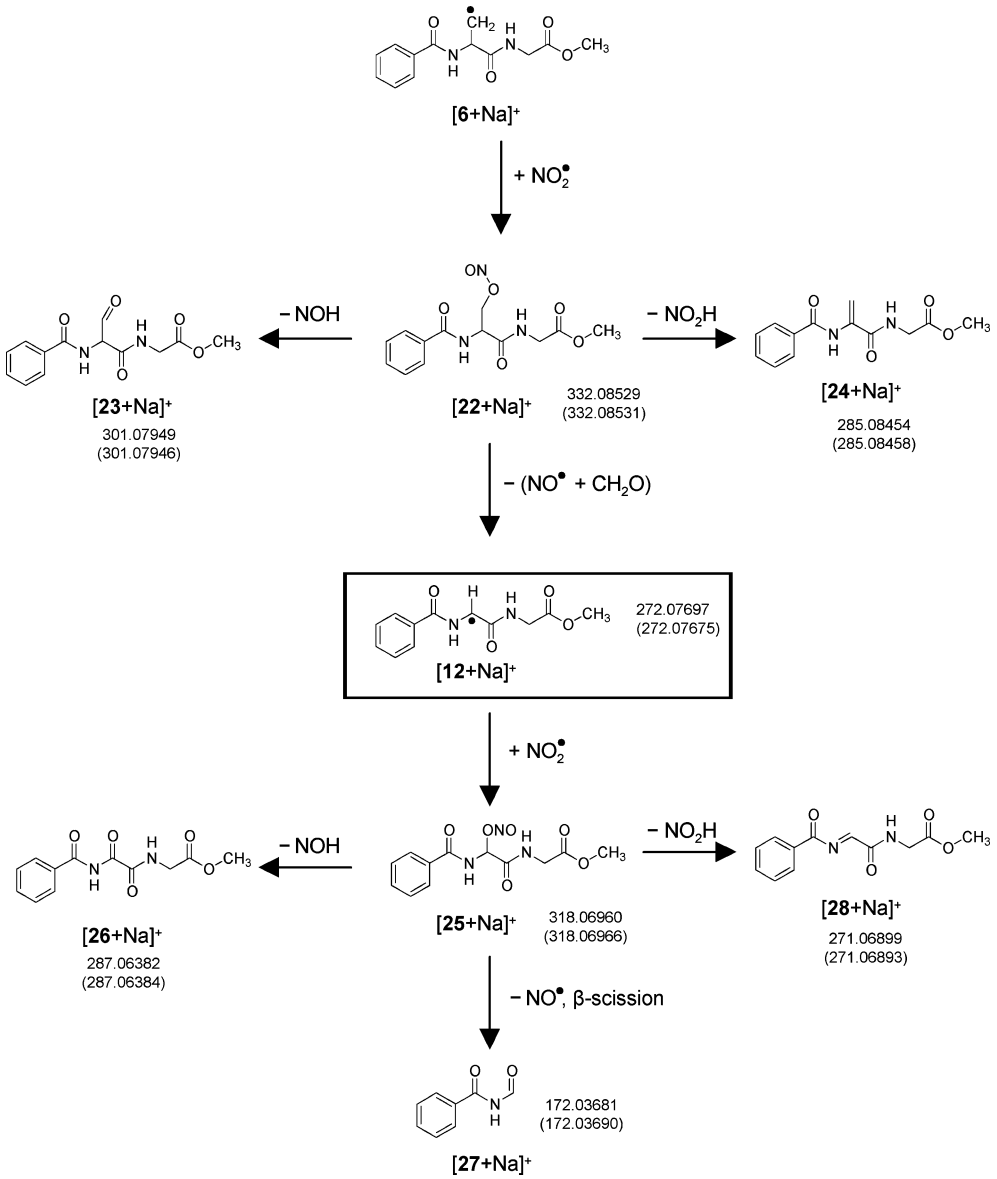

Scheme 6 Proposed structures arising from CID of [**22**+Na]$^+$, which was formed by addition of $NO_2^\bullet$ to [**6**+Na]$^+$. Experimental accurate masses are shown, with the corresponding theoretical masses in parentheses. Sodium ions have been excluded from structures for clarity. The primary fragment ion with a unique *m/z* value that is diagnostic of the [**6**+Na]$^+$ precursor is highlighted by a box.

stable radical product. Similarly, the alkyl hydroperoxide [**8**+Na]$^+$ decomposes upon CID *via* elimination of the HO$^\bullet$ radical to afford a transient alkoxyl intermediate, which undergoes β-scission to afford the stable C$^\alpha$-centred radical [**12**+Na]$^+$ (Scheme 3). Loss of NO$^\bullet$ from the nitrite ester [**22**+Na]$^+$ yields the identical intermediate (Scheme 6). These findings mirror previous solution phase work, which has demonstrated that C-3 alkoxyl radicals undergo rapid β-scission to afford a stable backbone C$^\alpha$-radicals.[38] Failure to directly observe the alkoxyl radical intermediate in our experiments is consistent with the rapid nature of β-scission. Critically, the decomposition of these C$^\beta$-alkoxyl radicals provides a means by which a radical initially at a side-chain may be transferred to the C$^\alpha$ of the peptide backbone from which backbone cleavage is known to occur.

C$^\alpha$-Alkoxyl radical intermediates are also implicated as intermediates in the oxidative cleavage of peptide backbones brought about by initial radical formation at the C$^\alpha$ of the peptide backbone followed by formation of hydroperoxides. In these cases β-scission occurs *via* cleavage of the C–C bond in the peptide backbone. Although, the extent of O_2 addition was too low to enable us to form α-hydroperoxide species in our current investigation, the C$^\alpha$-alkoxyl intermediates were implicated in the dissociation of the nitrite esters [**13**+Na]$^+$ and [**17**+Na]$^+$ formed upon addition of $NO_2^\bullet$ to the C$^\alpha$-radicals [**4**+Na]$^+$ and [**5**+Na]$^+$. Consistent with previous solution-phase studies as well as recent theoretical studies[51] we similarly observe β-scission of the backbone C–C bond (to form [**16**+Na]$^+$ in Scheme 4, [**20**+Na]$^+$ in Scheme 5 and [**27**+Na]$^+$ in Scheme 6).

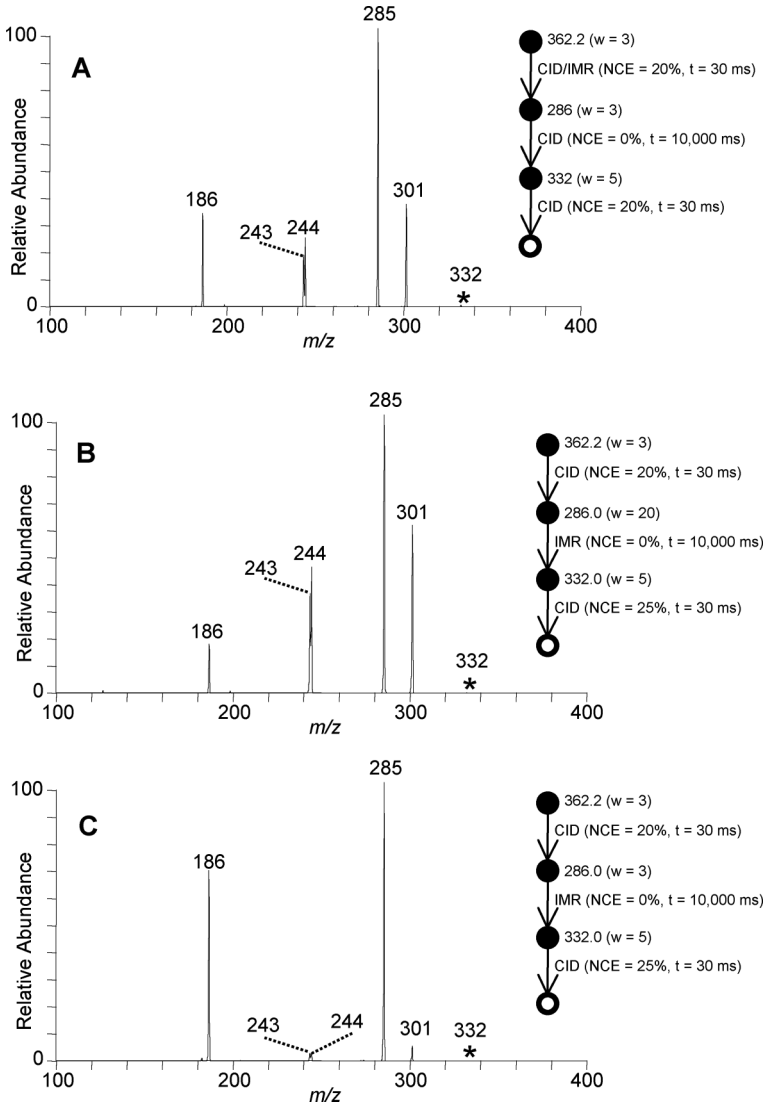

Fig. 6 Use of NO_2 as a radical trap to probe the isomerisation of peptide radicals *via* intramolecular HAT. Spectra should be compared with those shown in Fig. 5. CID spectra of the NO_2 adducts at *m/z* 332 formed from: (**A**) reaction of NO_2 with the mass selected radical [**6**+Na]$^+$ (*m/z* 286) which was isolated with a narrow isolation width (w = 3) (in comparison to the CID spectrum of [**6**+Na+NO_2]$^+$ (Fig. 5C) the characteristic ion at *m/z* 272 is absent; ions at *m/z* 186, 243 and 244 are consistent with isomerisation of [**6**+Na]$^+$ to [**4**+Na]$^+$ (compare Fig. 5A) and [**5**+Na]$^+$ (compare Fig. 5B)); (**B**) reaction of NO_2 with the mass selected radical [**5**+Na]$^+$ (*m/z* 286) which was isolated with a wide isolation width (w = 20); and (**C**) reaction of NO_2 with the mass selected radical [**5**+Na]$^+$ (*m/z* 286) which was isolated with a narrow isolation width (w = 3). These demonstrate that the amount of isomerisation of the peptide radical [**5**+Na]$^+$ to [**4**+Na]$^+$ increases as the isolation width decreases.

Conclusions

A range of previous reports and the current work clearly show that gas-phase studies on charged peptide radicals provide insights into fundamental unimolecular and bimolecular reactivity. Recent work has shown that sulfhydryl radicals readily react with allyl halides and dimethyl disulfide, making these reagents useful probes for these radical sites in peptides.[32] The current work highlights that simple reagent gases such as O_2, NO$^\bullet$ and $NO_2^\bullet$ may also be useful structural probes for mass spectrometry-based studies of charged carbon-centred peptide radicals. Indeed $NO_2^\bullet$ appears to be an ideal choice for a gas-phase radical trap due to the following features: (i) it can readily be introduced *via* a seeded bath gas into a variety of mass spectrometers without the need for instrumental modifications; (ii) it is highly selective for radical ions (no addition has been observed with even electron counterpart ions); and (iii) the resulting nitrite adducts can be subject to CID, which gives rise to product ions in which information about the initial position of the radical may be inferred (*e.g.*, loss of NO$^\bullet$ followed by β-scission of the C–C backbone bonds provides ready evidence for C$^\alpha$-radicals). In the current study, this latter characteristic has allowed us to probe the details of intramolecular hydrogen atom migration leading to the interconversion of the sodiated peptide radicals.

Acknowledgements

CJE and RAJO thank the ARC for financial support *via* the ARC Centre of Excellence in Free Radical Chemistry and Biotechnology. We thank: Adam Mortimer for help with synthesis of the

peptides; Associate Professor Stephen Blanksby for discussions on the formation and reactivity of peroxyl radicals; and the referees for useful comments.

References

1 The full interview is available online from the Australian Academy of Science "Interviews with Australian Scientists" (accessed 10 December 2010): http://www.science.org.au/scientists/interviews/b/ab.html#9.
2 M. J. Davies, *Biochim. Biophys. Acta, Proteins Proteomics*, 2005, **1703**, 93–109.
3 K. J. Davies, *J. Biol. Chem.*, 1987, **262**, 9895–9901.
4 A. Rauk, *Chem. Soc. Rev.*, 2009, **38**, 2698–2715.
5 M. A. Lam, D. I. Pattison, S. E. Bottle, D. J. Keddie and M. J. Davies, *Chem. Res. Toxicol.*, 2008, **21**, 2111–2119.
6 W. M. Garrison, *Chem. Rev.*, 1987, **87**, 381–398.
7 C. L. Hawkins and M. J. Davies, *Biochim. Biophys. Acta, Bioenerg.*, 2001, **1504**, 196–219.
8 J. Neuzil, J. M. Gebicki and R. Stocker, *Biochem. J.*, 1993, **293**, 601–606.
9 P. Neta, R. E. Huie and A. B. Ross, *J. Phys. Chem. Ref. Data*, 1990, **19**, 413–513.
10 C. Von, Sonntag and H.-P. Schuchmann, In *Peroxyl Radicals*, Z. B Alfassi Ed., Wiley, New York, 1997, 173–234.
11 O. J. Mieden, M. N. Schuchmann and C. von Sonntag, *J. Phys. Chem.*, 1993, **97**, 3783–3790.
12 R. C. White and M. D. E. Forbes, *Org. Lett.*, 2006, **8**, 6027–6030.
13 M. L. Huang and A. Rauk, *J. Phys. Org. Chem.*, 2004, **17**, 777–786.
14 D. G. Watson, C. Atsriku and E. J. Oliveira, *Anal. Chim. Acta*, 2003, **492**, 17–47.
15 C. Fonseca, M. R. Domingues, C. Simões, F. Amado and P Domingues, *J. Mass Spectrom.*, 2009, **44**, 681–693.
16 R. Hodyss, H. A. Cox and J. L. Beauchamp, *J. Am. Chem. Soc.*, 2005, **127**, 12436–12437.
17 D. S. Masterson, H. Yin, A. Chacon, D. L. Hachey, J. L. Norris and N. A. Porter, *J. Am. Chem. Soc.*, 2004, **126**, 720–721.
18 A. Chacon, D. S. Masterson, H. Yin, D. C. Liebler and N. A. Porter, *Bioorg. Med. Chem.*, 2006, **14**, 6213–6222.
19 S. Wee, A. Mortimer, D. Moran, A. Wright, C. K. Barlow, R. A. J. O'Hair, L. Radom and C. J. Easton, *Chem. Commun.*, 2006, 4233–4235.
20 G. Hao and S. S. Gross, *J. Am. Soc. Mass Spectrom.*, 2006, **17**, 1725–1730.
21 V. Ryzhov, A. K. Y. Lam and R. A. J. O'Hair, *J. Am. Soc. Mass Spectrom.*, 2009, **20**, 985–995.
22 A. Lam, V. Ryzhov and R. A. J. O'Hair, *J. Am. Soc. Mass Spectrom.*, 2010, **21**, 1296–1312.
23 T. Ly and R. R. Julian, *Angew. Chem., Int. Ed.*, 2009, **48**, 7130–7137.
24 T. Ly and R. R. Julian, *J. Am. Chem. Soc.*, 2008, **130**, 351–358.
25 Z. Liu and R. R. Julian, *J. Am. Soc. Mass Spectrom.*, 2009, **20**, 965–971.
26 I. K. Chu, J. Zhao, M. Xu, S. O. Siu, A. C. Hopkinson and K. W. M. Siu, *J. Am. Chem. Soc.*, 2008, **130**, 7862–7872.
27 C.-K. Siu, J. Zhao, J. Laskin, I. K. Chu, A. C. Hopkinson and K. W. M. Siu, *J. Am. Soc. Mass Spectrom.*, 2009, **20**, 996–1005.
28 Q. Sun, H. Nelson, T. Ly, B. M. Stoltz and R. R. Julian, *J. Proteome Res.*, 2009, **8**, 958–966.
29 B. N. Moore, S. J. Blanksby and R. R. Julian, *Chem. Commun.*, 2009, 5015–5017.
30 S. J. Ye and P. B. Armentrout, *J. Phys. Chem. A*, 2008, **112**, 3587–3596.
31 H. I. Kenttämaa, "Ion-molecule Reactions of Distonic Radical Cations," in *Encyclopedia of Mass Spectrometry, Volume 4: Fundamentals of and Applications to Organic (and Organometallic) Compounds*, N. N. M. Nibbering, Volume Ed., M. L. Gross and R. Caprioli, ed., Elsevier: New York, 2005, 160–165.
32 S. Osburn, J. D. Steill, J. Oomens, R. A. J. O'Hair, M. V. Stipdonk and V. Ryzhov, *Chem.–Eur. J.*, 2011, **17**, 873–879.
33 A. L. J. Beckwith and B. S. Low, *J. Chem. Soc.*, 1961, 1304–1311.
34 A. L. J. Beckwith and B. S. Low, *Aust. J. Chem.*, 1963, **16**, 845–853.
35 A. L. J. Beckwith, A. G. Davies, I. G. E. Davison, A. Maccoll and M. H. Mruzek, *J. Chem. Soc., Perkin Trans. 2*, 1989, 815–824.
36 A. L. J. Beckwith, A. G. Davies, I. G. E. Davison, A. Maccoll and M. H. Mruzek, *J. Chem. Soc., Chem. Commun.*, 1988, 475–476.
37 C. J. Easton, A. J. Ivory and C. A. Smith, *J. Chem. Soc., Perkin Trans. 2*, 1997, 503–507.
38 H. A. Headlam, A. Mortimer, C. J. Easton and M. J. Davies, *Chem. Res. Toxicol.*, 2000, **13**, 1087–1095.
39 G. E. Reid, R. A. J. O'Hair, M. L. Styles, W. D. McFadyen and R. J. Simpson, *Rapid Commun. Mass Spectrom.*, 1998, **12**, 1701–1708.
40 T. Waters, R. A. J. O'Hair and A. G. Wedd, *J. Am. Chem. Soc.*, 2003, **125**, 3384–3396.
41 J. C. Schwartz, A. P. Wade, C. G. Enke and R. G. Cooks, *Anal. Chem.*, 1990, **62**, 1809–18.
42 Y. Xia, P. A. Chrisman, S. J. Pitteri, D. E. Erickson and S. A. McLuckey, *J. Am. Chem. Soc.*, 2006, **128**, 11792–11798.
43 D. G. Harman and S. J. Blanksby, *Chem. Commun.*, 2006, 859–861.
44 D. G. Harman and S. J. Blanksby, *Org. Biomol. Chem.*, 2007, **5**, 3495–3503.
45 B. B. Kirk, D. G. Harman and S. J. Blanksby, *J. Phys. Chem. A*, 2010, **114**, 1446–1456.
46 ADO rate constant were calculated using: K. F. Lim, Quantum Chemistry Program Exchange, 1994, The program Colrate (1994) is available for download from author's website at Deakin University, Geelong, Victoria, Aus. http://www.deakin.edu.au/~lim/programs/COLRATE.html.
47 H. G. Viehe, Z. Janousek, R. Merenyi and L. Stella, *Acc. Chem. Res.*, 1985, **18**, 148–54.
48 Y.-R. Luo, *Handbook of Bond Dissociation Energies in Organic Compounds*, CRC Press, Boca Raton, Florida, 2003.
49 R. Asatryan, J. W. Bozzelli and J. M. Simmie, *J. Phys. Chem. A*, 2008, **112**, 3172–3185.
50 R. G. Cooks, D. Zhang, K. J. Koch, F. C. Gozzo and M. N. Eberlin, *Anal. Chem.*, 2001, **73**, 3646–3655.
51 G. P. F. Wood, C. J. Easton, A. Rauk, M. J. Davies and L. Radom, *J. Phys. Chem. A*, 2006, **110**, 10316–10323.